Cell wall biochemical alterations during Agrobacterium -mediated expression of haemagglutinin-based influenza virus-like vaccine particles in tobacco

François Le Mauff, Corinne Loutelier-Bourhis, Muriel Bardor, Caroline Berard, Alain Doucet, Marc-André d'Aoust, Louis-Philippe Vezina, Azeddine Driouich, Manon M.-J. Couture, Patrice Lerouge

Received Date : 30-Mar-2016
Revised Date : 18-Jul-2016
Accepted Date : 24-Jul-2016
Article type : Research Article

Cell wall biochemical alterations during *Agrobacterium*-mediated expression of hemagglutinin-based influenza virus-like vaccine particles in tobacco

François LE MAUFF[1,2,*], Corinne LOUTELIER-BOURHIS[3], Muriel BARDOR[1], Caroline BERARD[4], Alain DOUCET[2], Marc-André D'AOUST[2], Louis-Philippe VEZINA[2,#], Azeddine DRIOUICH[1], Manon M-J. COUTURE[2] and Patrice LEROUGE[1]

[1] Normandie Univ, UNIROUEN, laboratoire Glyco-MEV EA 4358, 76000 Rouen, France.

[2] Medicago inc., 1020 Route de l'Eglise, Québec, QC G1V 3V9, Canada.

[3] Normandie Univ, UNIROUEN, CNRS UMR 6014, Laboratoire COBRA, 76000 Rouen, France.

[4] Normandie Univ, UNIROUEN, LITIS EA 4108, 76000 Rouen, France.

Corresponding author: Patrice LEROUGE, Laboratoire Glyco-MEV EA4358, Institut de Recherche et d'Innovation Biomédicale, Normandie Université, 76821 Mont-Saint-Aignan, France. Telephone: 33 2 35 14 63 94; Fax number: 33 2 35 14 66 15; e-mail: patrice.lerouge@univ-rouen.fr

Key words: cell wall, virus-like particle, plant, Agrobacterium, tobacco, Hemagglutinin

This article has been accepted for publication and undergone full peer review but has not been through the copyediting, typesetting, pagination and proofreading process, which may lead to differences between this version and the Version of Record. Please cite this article as doi: 10.1111/pbi.12607

Running title: VLP production induces plant cell wall alterations

Summary

Influenza virus-like particles (VLPs) have been shown to induce a safe and potent immune response through both humoral and cellular mechanisms. They represent promising novel influenza vaccine. Plant-based biotechnology allows for the large-scale production of VLPs of biopharmaceutical interest using different model organisms, including *Nicotiana benthamiana* plants. In this platform, influenza VLPs bud from the plasma membrane and accumulate between the membrane and the plant cell wall. A better understanding of the plant cell wall composition of infiltrated tobacco leaves becomes a major interest for the plant-biotechnology industry in order to design and optimize efficient production processes. In this study, we have investigated the alteration of the biochemical composition of cell walls from *N. benthamiana* leaves subjected to abiotic and biotic stresses induced by the *Agrobacterium*-mediated transient transformation and the high-level expression of influenza VLPs. By comparison with non-infiltrated leaves, results show that abiotic stress due to vacuum infiltration without *Agrobacterium* did not induce any detectable modification of the cell wall. In contrast, various chemical changes of the leaf cell walls were observed post *Agrobacterium* infiltration. Moreover, infection with *Agrobacterium* induced deposition of callose and lignin as well as modification of pectin methylesterification, increase of arabinosylation of RG-I side chains and expression of arabinogalactan proteins (AGPs). Finally, modifications of the cell wall composition in response to agro-infiltration were slightly more important in plants expressing hemagglutinin-based VLP than in plants infiltrated with the *Agrobacterium* strain containing the p19 suppressor of silencing alone.

Introduction

The market share of vaccines is rapidly increasing with a growing interest toward virus-like particles (VLPs) products. VLPs are produced by recombinant expression in heterologous systems of viral structural proteins. They mimic viruses with respect to their morphology and size as well as their immunogenic potential, but do not contain viral DNA or RNA constituting an important safety advantage over traditional vaccines (Grgacic and Anderson, 2006; Lua et al., 2014; Le Mauff et al., 2014). The last two decades witnessed the rise of plant biotechnology and demonstrated the potential of plant-derived biopharmaceuticals production platforms. Stable or transient expression of proteins in plants allows the production of well-folded and functional biopharmaceuticals, including VLPs, in a safe and scalable manner (Kushnir et al., 2012). After synthesis, hemagglutinin-based VLPs remain trapped in leaves within the apoplast space surrounded by the cell wall (D'Aoust *et al.* in 2010). Since agro-infiltration-based production of VLPs requires *Agrobacterium tumefaciens* as a vehicle for gene shuttling to the host cell nucleus, studying the impact of *Agrobacterium* infiltration on plant tissues composition is of primary importance. In this context, limited knowledge exists on the cell wall modifications occurring during transient expression although the bacterial plant-*Agrobacterium* interaction is well-understood (Pitzschke and Hirt, 2010; Pruss et al., 2008). Therefore, understanding the cell wall biochemical modification in tobacco leaves during the production process is of main interest.

Plant cell wall is composed of three main polymers: cellulose, hemicellulose and pectins. The cellulose is a polymer of β(1,4)-glucose that constitutes the main network of the cell wall ensuring anisotropic growth of cells (Baskin and Jensen, 2013; Brown, 2004). Hemicelluloses encompass polymers consisting of β(1,4)-linked

monosaccharides substituted by various side chains. Among them, xyloglucans are the most abundant hemicellulose in primary cell walls of eudicots. They consist of a cellulose backbone substituted by α(1,6)-linked xylose residues and additional arabinose, galactose or fucose units (Pena et al., 2008). Acetylesterifications occur either on carbone 6 of the glucose backbone, of the galactose or arabinose residues of the side chains (Gille et al., 2011). The xylans and mannans hemicelluloses are much less abundant in eudicots and do not exceed 5% of total hemicellulloses (Scheller and Ulvskov, 2010). Finally, pectins are acidic polymers of cell wall consisting of α(1,4)-linked homogalacturonan (HG) and rhamnogalacturonans (RG). HG presents different levels of methyl- and acetylesterification that varies according to plant development stage (Wolf et al., 2009). RG is further subdivided into two classes: RG-I which consists of arabinan and galactan chains linked to a backbone of [→2)-α-L-Rha*p*-(1→4)-α-D-Gal*p*A-(1→] repeating disaccharides (Mohnen, 2008) and RG-II which possess a homogalacturonan backbone that is substituted with four complex and structurally conserved oligosaccharide side chains (O'Neill, 2001). In addition to these polysaccharides, cell walls contain hydroxyproline rich glycoproteins (HRGP) (Nguema-Ona et al., 2013), such as arabinogalactan proteins (AGPs), and structural proteins.

Infections of plants by pathogens induce a large set of plant defense responses including deposition of lignin and callose as well as cross-linking between cell wall polysaccharides and glycoproteins (Malinovsky et al., 2014). These chemical modifications reinforce the walls of cells surrounding the infection site, creating a barrier that limits the spread of the pathogen (Zhao and Dixon, 2014). To date, modifications of cell wall polymers under biotic stress conditions are well described (Malinovsky et al., 2014). For example, relationship between defense signal

pathways, such as the jasmonic acid pathway, and modification of cellulose synthesis and lignification has been clearly demonstrated (Caño-Delgado et al., 2003). Moreover, xylan networks are known to be reinforced during infection through the cross-linking of ferrulate esters with lignins (Malinovsky et al., 2014). Pectins also play a key function as sentinel of the cell wall integrity. In the context of pathogen-plant interactions, pathogen and plant pectin-degrading enzymes release partially methylesterified oligogalacturonide fragments that act as signals of tissue infection by pathogens (Bethke et al., 2014).

In this paper, we present the biochemical alterations of the plant cell wall *N. benthamiana* plants arising from abiotic stress resulting from the vacuum infiltration and biotic stresses caused by infiltration of *Agrobacterium* or due to the transient expression of influenza-VLPs.

Results

Experimental design

Four *N. benthamiana* plant groups were submitted to different abiotic and biotic stresses in order to analyse their respective impact on plant cell wall constituents (Figure 1A). Sugar composition and linkage analyses of cell walls prepared from agro-infiltrated and non-infiltrated *N. benthamiana* plants were carried out in order to investigate the influence of *Agrobacterium*-mediated influenza VLP production on the cell wall composition (Figure 1B). Cell walls prepared from non-infiltrated (Ni) plants that were subjected to the same conditions as for the three other groups, were analysed and considered as a non-infiltrated control group, while cell walls of plants infiltrated with water only (Water) were studied to investigate the impact of the abiotic

stress due to the vacuum treatment used to infiltrate the *Agrobacterium* inside plant tissues. A third group of plants were agro-infiltrated with an *Agrobacterium* strain carrying a binary plasmid designed for the expression of the p19 suppressor of gene silencing, to assess biotic stress due to *Agrobacterium* infection (labelled as "p19" plants) in absence of VLP expression. Finally, a last plant group, annotated as "H5", was infiltrated with an *Agrobacterium* strain capable of transferring both p19 and the *Influenza* H5 hemagglutinin genes to the plant cells allowing for transient expression of the hemagglutinin and budding of VLP to occur (Figure 1A). For each group, leaves from three plants were harvested at day 1, 4 and 7 post-infiltration and the different cell wall components were sequentially extracted as follow: Alcohol Insoluble Residues (AIR) were first prepared and mainly consisted of cell wall polysaccharides and AGPs. Then, water-soluble constituents (pectins and AGPs) and hemicellulose fractions were extracted from the AIR fraction of each plant. Finally, insoluble material left was considered as being insoluble cellulose (Figure 1B).

Overall sugar composition of crude cell walls extracts (AIR)

Monosaccharide composition of AIR isolated from cell walls of non-infiltrated *N. benthamiana* leaves (Ni) was in agreement with previous data (Figure 2A) (Nguema-Ona et al., 2012) showing that glucose, galacturonic acid and rhamnose are the most abundant monosaccharides. Similar monosaccharide compositions were measured in AIR isolated from Water, P19 and H5 infiltrated leaves, collected from day 1 to day 7 (Supplemental Table 1). Sugar linkage composition of neutral monosaccharides, identified by gas chromatography coupled to an electron impact mass spectrometer (GC-EIMS) after permethylation of the sample, was first determined in Ni group. In the cell wall AIR fraction of these plants, the most

abundant partially methylated alditol acetate derivatives, were assigned to 4-linked glucose, 4,6-linked glucose, 2- and/or 4-linked xylose and terminal xylose derived from cellulose and xyloglucans (Figure 2B). Detection of 2-linked rhamnose and 2,4-linked rhamnose residues in a 2/1 ratio indicated that a third of the [→2)-α-L-Rha*p*-(1→4)-α-D-Gal*p*A-(1→] repeating unit of the RG-I backbone of cell walls of *N. benthamania* leaves were substituted by side chains. Linkages of galactose and arabinose residues were consistent with the presence of branched 5-linked arabinans and 4-linked galactans (Figure 2B).

The three main cell wall fractions, pectins, hemicelluloses and cellulose, isolated from AIR, were quantified for each plant group. The relative abundance of pectins, hemicellulose and cellulose components varied from 53 to 65%, from 12 to 28% and from 18 to 26%, respectively. No statistical significant differences were observed between control (Ni) and water, p19 and H5 infiltrated plants collected at day 1, 4 and 7 (Figure 2C).

Together, monosaccharide composition and sugar linkages analyses indicated that no major overall change in the cell wall polysaccharide compositions are occurring over the 7-day incubation period in infiltrated plants expressing H5 VLP, when compared to the control groups subjected to different stresses (Ni, Water and P19). The plant cell wall fractions were further analysed to investigate whether subtle modifications were induced by the different plant treatments.

Analysis of pectins and AGPs

Monosaccharide composition of polysaccharides extracted in hot water was further investigated to determine if the different infiltration treatments could induce subtle structural modifications that could not be revealed from the analysis of overall AIR fractions. This hot-water soluble fraction mainly contained pectins and AGPs of the

cell wall. Figure 3A presents the monosaccharide composition obtained for the Ni plant group at day 1. Galacturonic acid (GalA) was the main monosaccharide present in this fraction, followed by galactose (Gal), arabinose (Ara) and rhamnose (Rha). This indicated that pectins were mainly constituted of RG-I and homogalacturonans. Other pectic polysaccharides, such as RG-II and xylogalacturonans, represented only tiny percent of total pectins extracted and were not further analyzed.

Quantification of AGP was carried out by rocket gel electrophoresis showed that AGPs represented only 1.5 to 3% (w/w) of the water soluble fractions (Figure 3B). Furthermore, as shown in the figure 3B, the proportion of AGPs was found to increase by 2-fold for H5-infiltrated leaves when compared to Ni and water group. The contribution of the AGP to the monosaccharide composition was therefore revealed to be quite low. In consequence, monosaccharides detected in the hot-water soluble fraction mainly arise from pectins.

Sugar composition of the pectins extracted in the hot-water soluble fractions showed slight variations between tobacco leaf groups and over time. To better understand and illustrate these observations, three different ratios were calculated from the relative amount of the main sugars components: the GalA/Rha ratio reflects the proportion between RG-I and HG as these two monosaccharides are unique monomers of these respective pectin backbones, whereas ramification sizes of RG-I can be represented by the ratio between Ara or Gal (monosaccharides present in the side chains) relative to Rha residues (constituent of the RG-I backbone). GalA/Rha ratio indicated that RG-I and HG were in similar amounts in pectin extracts of all the plant groups with ca 58% of RG-I and 42% of HG. In contrast, Gal/Rha and Ara/Rha ratios changed over time or among the plant groups. Indeed, the Gal/Rha increased

from day 1 to day 7 but this variation is similar in the different plant groups and likely revealed the increase of galactan ramifications of the RG-I during the growth of plants over the 7-day incubation period (Figure 3C, left panel). In contrast, the increases of Ara/Rha ratio were observed only in agro-infiltrated leaves (p19 and H5) and not in the Ni leaves nor in the leaves infiltrated with water (Figure 3C, right panel). Moreover, this increase was more important in leaves expressing hemagglutinin-based VLP (H5). It was then concluded that infiltration with *Agrobacterium* strains induces an increase of arabinosylation of cell wall RG-I constituent, increase even higher when the hemagglutinin-based VLP is expressed.

Pectins are usually methyl- and/or acetyl-esterified. Degrees of acetylesterification and methylesterification were therefore measured in the different pectin fractions. No modification of the level of acetylation was detected suggesting that acetylesterification of pectins was not affected by any of the treatment performed (data not shown). As shown in Figure 3D, overall degree of methylesterification of the pectin was ca 15% and remained constant over the 7-day incubation period in Ni, water and p19 groups. Interestingly, this level of methylesterification slightly decreased from 15% to 11% over the same incubation period for the H5 group.

Analysis of hemicelluloses

Monosaccharide compositions of hemicellulose fractions from AIR extracted from the four plant groups over time were investigated. In addition, fragments of hemicelluloses released by digestion with specific endoglycanases were analysed by Matrix-Assisted Laser Desorption Ionization-Time of Flight-Mass Spectrometry (MALDI-TOF MS). This approach produces enzyme-specific fingerprints which allow

for a fast and informative monitoring of hemicellulose structural variations (Lerouxel et al., 2002). Sugar composition of hemicellulose indicated that the main monosaccharides found were glucose (Glc), xylose (Xyl) and arabinose (Ara), in a 5:2:1 ratio (Figure 4A) as expected according to literature (York et al., 1996). Moreover, this ratio remained constant in the different groups studied as well as at all the time points.

Presence of xylans was investigated by digesting hemicellulose extracts with an endoxylanase, and analysing the resulting xylan fragments by MALDI-TOF MS. No fragment corresponding to the xylan fingerprint was detected indicating that these hemicelluloses are in trace amounts in *N. benthamiana* cell wall (data not shown). In contrast, as illustrated in Figure 4B, digestion of the hemicellulose fractions with an endoglucanase, that cleaves xyloglucan after non-substituted glucose residues, released three main fragments for which masses were assigned to XXG, XSG and XSGG/GXSG, in agreement with data reported in the literature (Chevalier et al., 2010; Sims et al., 1996; York et al., 1996). These fragments were named according to the nomenclature suggested by Fry *et al.* (1993) where G refers to glucose units of the backbone, X and S refer to α-D-Xyl*p*-(1→6) and to α-L-Ara*f*-(1→2)-α-D-Xylp-(1→6) xyloglucan side chains, respectively (Figure 4D). The same enzyme fingerprinting analyses were performed on hemicellulose fractions isolated from leaves of plants harvested at day 1, 4 and 7. No detectable modification of monosaccharide composition and MALDI-TOF MS profiles was observed across the different plant groups (Supplemental Table 2A).

To investigate the presence of alkali labile substitutions on xyloglucan, endoglucanase digestion was performed on AIR fractions. In these conditions, endoglucanase releases fragments from native xyloglucan carrying alkali labile

groups that are otherwise lost during hemicellulose extraction with 4 M KOH. MALDI-TOF MS analysis of the digests showed xyloglucan fragments carrying one or two acetate groups (+ 42 Da) and larger oligoglucosyl backbones (Figure 4C, first panel, Supplemental Table 2B) (Chevalier et al., 2010; Sims et al., 1996). The presence of these fragments indicated that acetylation occurs on glucose residues that protects the backbone from exhaustive endoglucanase digestion. Based on these data, it was concluded that xyloglucan from *N. benthamania* cell wall leaves mainly consists of XXGGG repeating units that are substituted on xylose side chains by arabinose residues and acetylated on the backbone glucose residues (Figure 4D). The structure of major fragments was confirmed by analysis of fragmentation patterns obtained in tandem mass spectrometry (Supplemental Figure 1). Endoglucanase xyloglucan fingerprinting was carried out on AIR isolated from infiltrated leaves collected at day 1, 4 and 7 (Figure 4C). In the agro-infiltrated leaves (p19 and H5), minor ions were specifically and reproducibly detected in the m/z 1350-1450 range (Figure 4C). These ions were neither detected in control leaves, nor in leaves infiltrated with water, indicating that these additional xyloglucan fragments resulted from alkali labile modifications of xyloglucan in response to *Agrobacterium* infiltration. These ions, that are the unique modifications observed in xyloglucan fingerprints, did not significantly modify the xyloglucan overall structure and remain unidentified (Supplemental Tables 3B and 2C). Nevertheless, a significant increase of monolignols was observed in the xyloglucan-enriched fraction of H5 group at day 7 compared to Ni group at the same day (data not shown).

Callose and lignin deposition

Callose deposition was investigated by staining the tissue with aniline blue and observing the presence of callose under confocal microscope. As expected, this revealed that callose is synthesized in response to the agroinfiltration stress (not shown). To quantify the extent of callose deposition in infiltrated plants, 3-linked Glc was measured by GC-MS in leaves collected from day 7 plants. Permethylation of polysaccharides of AIR fractions allows the discrimination between 4-linked Glc derived from cellulose and 3-linked Glc found in callose only. Figure 5 shows the gas chromatography profiles of the monosubstituted hexoses obtained from day 7 leaves of Ni and water, or p19 or H5 infiltrated leaves. The results clearly demonstrated the presence of 3-linked Glc, and therefore reflect that callose is specifically synthesised in agro-infiltrated leaves (p19 and H5). Quantification of 3-linked Glc indicated that callose represented about 3% (w/w) of the cell wall polysaccharides in infected tissues of H5 VLP-expressing plants.

Lignin deposition was monitored by phloroglucinol staining of leaves. Infiltrations were carried out with a syringe on one half of the leaf; the other half remained untreated for comparison (Figure 6). Lignin deposition was detected as brown spots in agro-infiltrated leaves (p19 and H5) from day 4. At day 7, a more contrasted staining of all the infected tissues was observed relative to their respective controls non treated half leaf. In contrast, leaves infiltrated with water were comparable to control leaves demonstrating the specificity of the signal obtained.

Discussion

Plant-based biotechnology allows for the large-scale production of Influenza virus-like particles in *N. benthamiana* leaves through the *Agrobacterium*-mediated transient transformation and the expression of hemagglutinin surface protein. To investigate to what extent abiotic stress due to vacuum infiltration and/or biotic stress due to agro-infiltration induce cell wall modifications, chemical composition of cell walls from *N. benthamania* leaves was analysed, over a 7-day post infiltration period, in plants infiltrated under vacuum with different inoculum solutions (water, p19, H5) and results were compared to those of non-infiltrated plants. This study demonstrated that stresses induced by the infiltration process brought to large-scale for transient expression of considerable amount of biomass were not causing significant cell wall modification at the macromolecular level. All plant groups analysed showed a predominant portion of pectins in their cell wall and cellulosic compounds split equally between arabinoxyloglucans as the main hemicellulose, and cellulose, as it was expected for the *N. benthamiana* plants (Nguema-Ona et al., 2012, York et al., 1996). Observations of significant modifications were only possible after fractionation of the different polymers constituting the cell wall.

Looking at structural components of pectins, two main modifications were observed. The first one was a decrease in the methylesterification rate of the homogalacturonans. This process is already described in the literature and relies on the fact that during plant-pathogen interactions, homogalacturonan oligosaccharides are involved in the elicitation of the plant defense responses. Through the action of pectin-degrading enzymes, weakly methylesterified oligogalacturonides resulting from the degradation of homogalacturonans that are recognized by Wall-Associated Kinases receptors and induce defense gene expression (Ferrari et al., 2013; Osorio

et al., 2008). Moreover, de-esterification of galacturonic acid residues by pectin methylesterases is known to promote cell wall rigidification resulting in the cross linking of the acidic pectins with calcium ions, affecting the porosity of the primary cell wall and thus forming a stronger barrier to cross for pathogens (Peaucelle et al., 2012). The second modification observed on this polymer was on the ramifications of the rhamnogalacturonan. Analysis of the different ratio Ara/Rha and Gal/Rha exposed two different pectin responses. Galactosylation was shown to increase in relation with the growth of the plant as all the groups showed a significant increase of their proportion after the 4 and 7-days incubation time. Arabinosylation level of the rhamnogalacturonan side chains was increased in *Agrobacterium*-infiltrated leaves (P19 and H5 plants) by comparison to control plants. Such a cell wall modification in response to an *Agrobacterium* infection was not reported before. Elongation of RG-I arabinan chains during infection could reinforce the primary cell wall in response to infection as these side chains are known to interact with cellulose or xyloglucan (Wang et al., 2012; Zykwinska et al., 2005). Moreover, synthesis of arabinans may impact the flexibility of cell wall. Indeed, it was previously reported that, in an abiotic stress such as dehydration, arabinans are involved in the plant survival modulating the flexibility of the cell wall (Moore et al., 2008, 2013).

The level of AGP was also increased at day 7 in agro-infiltrated leaves by comparison to non-infiltrated plants. Although the involvement of AGPs in plant pathogen interaction has already been mentioned in the literature (Nguema-Ona et al., 2013; Seifert and Roberts, 2007), their precise role in the metabolic pathway of the plant defense against pathogens remains unclear. It was demonstrated that they can link pectins and hemicelluloses together and therefore may contribute to the cell wall rigidification, thus limiting the spread of the pathogens in the leaf tissue (Popper

and Fry, 2007; Tan et al., 2013). Another demonstration performed by Cannesan et al. in 2012 also established the involvement of the AGPs in plant defense reaction, highlighting the role of these molecules in the control of early infection of pea roots. In the industrial context of plant infection by *Agrobacterium*, the role of AGPs in the defense mechanisms remain unknown but our result exposed a potential role of these molecules in the leaf tissue as their population doubled over the 7-day infection.

Hemicelluloses in *N. benthamiana* cell wall are mainly composed of arabinoxyloglucans consisting of XXGGG repeating units that are substituted on xylose side chains by arabinose residues and acetylated on glucose residues of the backbone, in agreement with data reported for hemicelluloses from Solanaceae plants (Vincken et al., 1997; York et al., 1996). Enzymatic hydrolysis of AIR with endo-β-1.4-glucanase and MALDI-MS enzyme fingerprinting enabled the detection of numerous xyloglucan fragments carrying acetate groups. Comparison of MS profiles between the different plants groups did not show significant differences in the content of major fragments. Nevertheless, *Agrobacterium* infiltration induced the accumulation of three low abundant xyloglucan fragments that were not detected in control or water-infiltrated leaves and which structures remain unidentified. Since these fragments were no more observed after alkali treatments and considering that higher amounts of monolignols were detected in xyloglucan fractions, the hypothesis is that these stress-induced fragments could arise from the esterification of xyloglucan with monolignols. Such esterification has been reported for a dimer Xyl-α-1-6-Glc of arabinoxyloglucans by Ishii *et al.* in 1990. More experiments will have to be carried out to unravel the structures of these minor xyloglucan motifs and determine their function in plant defense against pathogens.

Callose and lignins polymers are known to be deposited in the cell wall during infections. These modifications are known to reinforce the walls of cells surrounding the infection site to limit the spread of the pathogen (Zhao et al., 2014). Callose accounted for up to 3% (w/w) of the cell wall polysaccharides in p19 and H5-infiltrated leaf groups. In addition, phloroglucinol staining revealed lignin deposition between the day 4 and the day 7 and only in leaves submitted to *Agrobacterium* infiltration treatments.

Comparison of cell walls of leaves collected from p19 and H5 plants indicated that expression of H5-VLP vaccines induced more important cell wall modification than those observed post-infiltration with *Agrobacterium* containing the inhibitor of gene silencing p19 sequence alone. This is mainly illustrated by data with regards to AGPs, degree of methylesterification and arabinan contents. These observations suggested that in addition to defense reactions related to the infection with *Agrobacterium* strains, accumulation of VLPs in leaves may induce an additional modification either due to a physical constraint related to HA accumulation or budding of VLP between the plasma membrane and the cell wall.

Altogether these data allow a better understanding of the modifications to plant cell wall composition in infiltrated tobacco leaves in the context of the production of influenza VLPs. The identified modifications are known to rigidify the cell wall and to alter its degradation by pathogens, it is therefore expected that these modifications have an impact on the mechanical and enzymatic extraction processes. As a further step towards an optimal extraction process, we are currently evaluating the impact of the modifications to cell wall composition on the efficacy of

the influenza VLP extraction process. The acquired knowledge of the cell wall structure and its defense-induced reinforcement will greatly help in designing optimal extraction processes for influenza VLPs and other biopharmaceutical proteins.

Experimental procedures

Materials

Eight week-old *N. benthamiana* plants were infiltrated under vacuum either with water or with *Agrobacterium tumefaciens* suspension containing a plasmid encoding for the silencing p19 alone or in combination to a gene sequence encoding the *Influenza* H5 hemagglutinin. At day 1, 4 and 7 following *Agrobacterium* infiltration, 12 plants were taken out of the green house, 3 corresponding to non-infiltrated plants as negative control group, 3 plants infiltrated with water and named water, 3 plants infiltrated with *Agrobacterium* containing the p19 gene sequence named “p19” and finally 3 plants infiltrated with *Agrobacterium* containing both p19 and H5 hemagglutinin gene sequences named “H5” (Figure 1A).

Preparation of Alcohol Insoluble Residues

Leaves were harvested and then crushed in 70% ethanol. In order to remove chlorophyll and pigments, successive incubations were performed in 70% ethanol at 70°C for 15 min and centrifugation at 4 500 g for 5 min at 4°C. Once pigments were completely removed from the samples, the insoluble materials were washed in methanol: chloroform (1: 1) and then in acetone. These successive washing steps led to isolation of insoluble samples named Alcohol Insoluble Residues (AIR) (Figure 1B).

Sequential extraction of cell wall polysaccharides

Pectins and AGPs were extracted from AIR fraction by incubation in water at 90°C and then in 0.5% oxalate ammonium at 90°C. Soluble fractions were separated from the insoluble materials by centrifugation at 5000 g, dialyzed against water for oxalate ammonium part and then lyophilized. Hemicelluloses were extracted from the previous insoluble residue with 4 M potassium hydroxide containing 0.1% sodium borohydride. Soluble fractions containing hemicelluloses were neutralized and dialyzed against water. Insoluble residues after 4 M KOH treatments correspond to insoluble cellulose.

Monosaccharide composition

Two mg of polysaccharide fractions were hydrolyzed with 2M trifluoroacetic acid (TFA) for 2 h at 110°C. After freeze-dring, samples were then converted in methyl glycosides by heating in 1 M methanol-HCl (Supelco) for 16 h at 80 °C. Samples were dried under a stream of nitrogen, washed twice with methanol and then treated with hexamethyldisilazane (HMDS) : trimethylchlorosilane (TMCS) : pyridine solution (3 : 1 : 9, Supelco), for 20 min at 80°C. The resulting trimethylsilyl methyl glycosides were dried, resuspended in 1ml of cyclohexane and injected in the 3800 GC system equipped of a CP-Sil5-CB capillary column (Agilent Technologies). Elution was performed with the following temperature gradient: 120°C to 160°C at a rate of 10°C/min, 160°C to 220°C at a rate of 1.5°C/min, 220°C to 280°C at a rate of 20°C/min. Quantification of each monosaccharides was carried out using standards and response factors determined for each monosaccharide.

Sugar linkage analysis

Five mg of AIR were permethylated with iodomethane in a suspension of NaOH in dry DMSO and the resulting partially methylated alditol acetate derivatives were prepared according to protocols described by the glycotechnology core resource of SanDiego (http://glycotech.ucsd.edu/protocols/07_Comp_Analysis_by_Alditol_Rev2.pdf). Monosaccharide derivatives were injected in a gas chromatograph (GC) (Hewlett-Packard 6890 series) coupled to an electron impact Autospec mass spectrometer (EI-MS) (Micromass, Manchester, UK) equipped with an Opus 3.1 data system. Separations were obtained using a Zebron Z5-MSi (30m, 0.25mm id, 0.25µm film thickness, Phenomenex) capillary column. Helium was the carrier gas and the flow-rate was 0.8mL/min. The temperature programming started at 100°C for 1 min, ramped to 160°C at 10°C/min, then ramped to 220°C at 2°C/min and finally ramped to 270°C at 15°C/min (maintained at 270°C for 1 min). The temperatures of the injector, the interface and the lines were 250°C. Injections of 0.5 µL were performed in splitless mode. EI mass spectra were recorded using electron energy of 70eV, an acceleration voltage of 8kV and a resolving power of 1000. The trap current of 200 µA and the magnet scan rate was 1s/decade over a m/z range 600-3800. The temperature of ion source was 250°C. Sugar linkage analysis was deduced from the EI-MS fragmentation patterns of partially methylated alditol acetate derivatives according to http://www.ccrc.uga.edu/databases/PMAA.

Determination of degree of methylesterification of pectins

Pectin fractions were saponified by 0.1M sodium hydroxide at 4°C during 2 h. Solutions were then neutralized by addition of 0.1M HCl and then used for Klavons titration. Five hundred µl of samples were diluted to 1 ml with 0.1M potassium

phosphate pH 7.5. One ml of alcohol oxidase 1U/ml was then added and the solution was incubated for 15 min at 25°C. Two ml of 0.02M 2.4-pentandione in 0.05M acetic acid and 0.2M ammonium acetate were added and the mixture was heated at 60°C for 15 min. Absorbance at 412nm was then recorded and converted into µg/ml of methanol with respect to a calibration curve.

Determination of degree of acetylesterification of pectins

Pectin acetylation was determined using a Megazyme acetic acid assay kit (E-ACETRM) after saponification of pectins and monitoring of released acetic acid according to the supplier instructions.

Xyloglucan fingerprinting

Two mg of AIR or hemicellulose fractions were digested with 4U of endo-beta-glucanase (Megazyme, Ireland), in sodium acetate buffer 0.01M pH 5 at 37°C overnight. After addition of 3 volumes of cold 100% ethanol, the soluble fraction containing xyloglucan fragments was collected by centrifugation at 5.000 g. Supernatant was dried and then dissolved in 100 µL of 0.1% TFA. One µL was spotted on a MALDI-TOF plate with DHB as matrix. Spectra were recorded on a Voyager DE-Pro from AB Sciex in positive reflector mode and accumulation of 3000 laser shots.

Xylan fingerprinting

Search for xylan fragments was done according to the protocol carried out for xyloglucan fingerprinting using ten µl of Xylanase M6 (Megazyme, Ireland) as endoglycanase.

AGP quantification

Soluble fraction resuspended at 9mg/ml were spotted on a 1% agarose gel containing Yariv reagent at 50µg/ml. Gel was then placed under 200V electric field overnight. Quantification was carried out using a calibration curve obtained with arabic gum displaced inside the gel. The area of trapped AGPs was calculated by ImageJ software.

Determination of lignin deposition

Lignin deposition was monitored by staining *N. benthamiana* leaves with phloroglucinol. Leaves were washed with 100% ethanol during 3 days in order to remove pigments. Then, leaves were incubated with 2.5% phloroglucinol in 70% ethanol overnight at room temperature. Revelation of the phloroglucinol staining was then performed by incubation in 37% hydrochloric acid during 5 min.

Quantification of phenolic compounds

In the xyloglucan-enriched fraction obtained after endoglucanase digestion precipitated with absolute ethanol, a silylation was performed through a treatment with BSTFA/TMCS (Supelco, Sigma Aldrich) in dry pyridine solvent for 30 minutes at 80°C. Samples were then dried and resuspended in cyclohexane before being injected in the same amount in gas chromatograph (GC) (Hewlett-Packard 6890 series) coupled to an electron impact Autospec mass spectrometer (EI-MS) (Micromass, Manchester, UK) equipped with an Opus 3.1 data system. Separations were obtained using a Zebron Z5-MSi (30m, 0.25mm id, 0.25µm film thickness, Phenomenex) capillary column. Helium was the carrier gas and the flow-rate was

0.8mL/min. The temperature programming started at 100°C for 1 min, ramped to 160°C at 10°C/min, then ramped to 220°C at 2°C/min and finally ramped to 270°C at 15°C/min (maintained at 270°C for 1 min). The temperatures of the injector, the interface and the lines were 250°C. Injections of 0.5 µL were performed in splitless mode. EI mass spectra were recorded using electron energy of 70eV, an acceleration voltage of 8kV and a resolving power of 1000. The trap current of 200 µA and the magnet scan rate was 1s/decade over a m/z range 600-3800. The temperature of ion source was 250°C. Identification of phenolic compound was based on the injection of standards of each of them. Quantification was then performed thanks to a ratio between area under curve of the peaks of interest and peak of xylose.

Statistical analysis

Statistical analysis were performed using the R software. The data were first normalized according to the experimental internal standard method, and then statistical tests were run on the basis of three biological replicates and three technical replicates. To study the evolution of the cell wall between the 4 different conditions and the 3 different days, an ANOVA were performed. Let Y_{cds} be the analyzed signal for the component *s*, condition *c* and the day *d*. Therefore, the model is: $Y_{cds} = \mu + \alpha_c + \beta_d + \gamma_{cd} + \varepsilon_{cds}$, where α_c is the condition factor, β_d is the day factor, γ_{cd} is the condition and day interaction, and ε_{cds} are the gaussian residues. The effect between the different plant groups was considered significant when a p-value lower than 0.05 was obtained. When p-value were under 0.05, Bonferroni post-tests were further performed to specify if the difference was coming from the condition factor, the day factor or from their synergy.

Acknowledgement: Authors would like to thank the University of Rouen and Medicago Inc. for their financial and scientific support. All authors declared they have no conflict of interest.

References

Baskin, T.I., and Jensen, O.E. (2013). On the role of stress anisotropy in the growth of stems. *J. Exp. Bot.* doi:10.1093/jxb/ert176.

Bethke, G., Grundman, R.E., Sreekanta, S., Truman, W., Katagiri, F., and Glazebrook, J. (2014). Arabidopsis pectin methylesterases contribute to immunity against Pseudomonas syringae. *Plant Physiol.,* **164**, 1093–1107.

Brown, R.M. (2004). Cellulose structure and biosynthesis: what is in store for the 21st century? *J. Polym. Sci. Part Polym. Chem.*, **42**, 487–495.

Caño-Delgado, A., Penfield, S., Smith, C., Catley, M., and Bevan, M. (2003). Reduced cellulose synthesis invokes lignification and defense responses in Arabidopsis thaliana. *Plant J.,* **34**, 351–362.

Chevalier, L., Bernard, S., Ramdani, Y., Lamour, R., Bardor, M., Lerouge, P., Follet-Gueye, M.-L., and Driouich, A. (2010). Subcompartment localization of the side chain xyloglucan-synthesizing enzymes within Golgi stacks of tobacco suspension-cultured cells. *Plant J.*, **64**, 977–989.

D'Aoust, M.-A., Couture, M.M.-J., Charland, N., Trépanier, S., Landry, N., Ors, F. and Vézina, L.-P. (2010) The production of hemagglutinin-based virus-like particles in plants: a rapid, efficient and safe response to pandemic influenza. *Plant Biotechnol.J.* **8**, 607–619.

Ferrari, S., Savatin, D.V., Sicilia, F., Gramegna, G., Cervone, F., and De Lorenzo, G. (2013). Oligogalacturonides: plant damage-associated molecular patterns and regulators of growth and development. *Plant Physiol.,* **4**, 49.

Fry SC, York WS, Albersheim P.(1993). An unambiguous nomenclature for xyloglucan-derived oligosaccharides. *Physiologia Plantarum,* **89**: 1–3.

Grgacic, E.V.L., and Anderson, D.A. (2006). Virus-like particles: Passport to immune recognition. *Methods*, **40**, 60–65.

Ishii T., Hiroi T., Thomas J.R. (1990). Feruloylated xyloglucan and p-coumaroyl-arabinoxylan oligosaccharides from bamboo shoot cell walls. *Phytochemistry.* **6**, 1999-2003.

Kushnir, N., Streatfield, S.J., and Yusibov, V. (2012). Virus-like particles as a highly efficient vaccine platform: Diversity of targets and production systems and advances in clinical development. *Vaccine*, **31**, 58–83.

Lerouxel, O., Choo, T.S., Séveno, M., Usadel, B., Faye, L., Lerouge, P., and Pauly, M. (2002). Rapid structural phenotyping of plant cell wall mutants by enzymatic oligosaccharide fingerprinting. *Plant Physiol.*, **130**, 1754–1763.

Le Mauff, F., Mercier, G., Chan, P., Burel, C., Vaudry, D., Bardor, M., Vézina, L.-P., Couture, M., Lerouge, P., and Landry, N. (2014). Biochemical composition of haemagglutinin-based influenza virus-like particle vaccine produced by transient expression in tobacco plants. *Plant Biotechnol. J.* doi:10.1111/pbi.12301.

Lua, L.H.L., Connors, N.K., Sainsbury, F., Chuan, Y.P., Wibowo, N., and Middelberg, A.P.J. (2014). Bioengineering virus-like particles as vaccines. *Biotechnol. Bioeng.,* **111**, 425–440.

Malinovsky, F.G., Fangel, J.U., and Willats, W.G.T. (2014). The role of the cell wall in plant immunity. *Front. Plant Sci.*, **5**.

Mohnen, D. (2008). Pectin structure and biosynthesis. *Curr. Opin. Plant Biol.*, **11**, 266–277.

Moore, J.P., Farrant, J.M., and Driouich, A. (2008). A role for pectin-associated arabinans in maintaining the flexibility of the plant cell wall during water deficit stress. *Plant Signal. Behav.*, **3**, 102–104.

Moore, J.P., Nguema-Ona, E.E., Vicré-Gibouin, M., Sørensen, I., Willats, W.G.T., Driouich, A., and Farrant, J.M. (2013). Arabinose-rich polymers as an evolutionary strategy to plasticize resurrection plant cell walls against desiccation. *Planta*, **237**, 739–754.

Nguema-Ona, E., Moore, J.P., Fagerström, A., Fangel, J.U., Willats, W.G.T., Hugo, A., and Vivier, M.A. (2012). Profiling the main cell wall polysaccharides of tobacco leaves using high-throughput and fractionation techniques. *Carbohydr. Polym.*, **88**, 939–949.

Nguema-Ona, E., Vicré-Gibouin, M., Cannesan, M.-A., and Driouich, A. (2013). Arabinogalactan proteins in root–microbe interactions. *Trends Plant Sci.*, **18**, 440–449.

O'Neill, M.A. (2001). Requirement of borate cross-linking of cell wall Rhamnogalacturonan II for Arabidopsis growth. *Science*, **294**, 846–849.

Osorio, S., Castillejo, C., Quesada, M.A., Medina-Escobar, N., Brownsey, G.J., Suau, R., Heredia, A., Botella, M.A., and Valpuesta, V. (2008). Partial demethylation of oligogalacturonides by pectin methyl esterase 1 is required for eliciting defense responses in wild strawberry (Fragaria vesca). *Plant J.*, **54**, 43–55.

Peaucelle, A., Braybrook, S. and Höfte, H. (2012). Cell wall mechanics and growth control in plants: the role of pectins revisited. *Frontiers in plant science*, **3**, 121.

Pena, M.J., Darvill, A.G., Eberhard, S., York, W.S., and O'Neill, M.A. (2008). Moss and liverwort xyloglucans contain galacturonic acid and are structurally distinct from the xyloglucans synthesized by hornworts and vascular plants. *Glycobiology*, **18**, 891–904.

Pitzschke, A., and Hirt, H. (2010). New insights into an old story: Agrobacterium-induced tumour formation in plants by plant transformation. *EMBO J.*, **29**, 1021–1032.

Popper, Z.A., and Fry, S.C. (2007). Xyloglucan–pectin linkages are formed intra-protoplasmically, contribute to wall-assembly, and remain stable in the cell wall. *Planta*, **227**, 781–794.

Pruss, G.J., Nester, E.W., and Vance, V. (2008). Infiltration with Agrobacterium tumefaciens induces host defense and development-dependent responses in the infiltrated zone. *Mol. Plant. Microbe Interact.*, **21**, 1528–1538.

Scheller, H.V., and Ulvskov, P. (2010). Hemicelluloses. *Annu. Rev. Plant Biol.*, **61**, 263–289.

Seifert, G.J., and Roberts, K. (2007). The biology of arabinogalactan proteins. *Annu. Rev. Plant Biol.,* **58**, 137–161.

Sims, I.M., Munro, S.L., Currie, G., Craik, D., and Bacic, A. (1996). Structural characterisation of xyloglucan secreted by suspension-cultured cells of Nicotiana plumbaginifolia. *Carbohydr. Res.*, **293**, 147–172.

Tan, L., Eberhard, S., Pattathil, S., Warder, C., Glushka, J., Yuan, C., Hao, Z., Zhu, X., Avci, U., Miller, J.S., et al. (2013). An Arabidopsis cell wall proteoglycan consists of pectin and arabinoxylan covalently linked to an arabinogalactan protein. *Plant Cell Online*, **25**, 270–287.

Vincken, J.-P., York, W.S., Beldman, G., and Voragen, A.G. (1997). Two general branching patterns of xyloglucan, XXXG and XXGG. *Plant Physiol.,* **114**, 9.

Wang, T., Zabotina, O., and Hong, M. (2012). Pectin-cellulose interactions in the Arabidopsis primary cell wall from two-dimensional magic-angle-spinning solid-state nuclear magnetic resonance. *Biochemistry*, **51**, 9846–9856.

Wolf, S., Mouille, G., and Pelloux, J. (2009). Homogalacturonan methyl-esterification and plant development. *Mol. Plant*, **2**, 851–860.

York, W.S., Kumar Kolli, V.S., Orlando, R., Albersheim, P., and Darvill, A.G. (1996). The structures of arabinoxyloglucans produced by solanaceous plants. *Carbohydr. Res.*, **285**, 99–128.

Zhao, Q., and Dixon, R.A. (2014). Altering the cell wall and its impact on plant disease: from forage to bioenergy. *Annu. Rev. Phytopathol.*, **52**, 1.

Zipfel, C., Kunze, G., Chinchilla, D., Caniard, A., Jones, J.D.G., Boller, T., and Felix, G. (2006). Perception of the bacterial PAMP EF-Tu by the receptor EFR restricts Agrobacterium-mediated transformation. *Cell*, **125**, 749–760.

Zykwinska, A.W., Ralet, M.-C.J., Garnier, C.D., and Thibault, J.-F.J. (2005). Evidence for in vitro binding of pectin side chains to cellulose. *Plant Physiol.,* **139**, 397–407.

Figure legends

Figure 1:

Experimental design of plants submitted to different biotic and abiotic treatments (A) and preparation of the cell wall constituents (B). Lightening icons represent the different stresses applied to each groups: abiotic stress from infiltration is in blue, biotic stress of bacterial infection is represented in green, and biotic stress arising from VLP production and accumulation is in red.

Figure 2:

Analysis of AIR material. Sugar composition (A) and linkages (B) analysis of main neutral monosaccharides of AIR extracted from control leaves at day 1. *co-eluting partially O-methylated samples. Relative percentages of cell wall polysaccharide fractions from all conditions at Day 1, 4 and 7 (C). Ara: arabinose, Rha: rhamnose, Fuc: fucose, Xyl: xylose, GlcA: glucuronic acid, Man: mannose, GalA: galacturonic acid, Gal: galactose, Glc: glucose, t-: terminal.

Figure 3:

Analysis of water soluble material. Monosaccharide composition of water soluble fraction of control plant at day 1 (A). Quantification of AGPs present in the water soluble fraction at day 7 (B). *: p-value below 0.05, **: p-value below 0.01 and ***: p-

value below 0.001. Gal/Rha (left panel) and Ara/Rha ratio (right panel). Day 1 in black, day 4 in grey and day 7 in white. Symbols below charts indicate statistical analysis between the different conditions. First symbol corresponds to analysis performed on day 1, second one on day 4 and last one on day 7 (C). 0: no difference, *: p-value below 0.05, **: p-value below 0.01 and ***: p-value below 0.001. Degrees of methylesterification of pectins (D).

Figure 4:

Analysis of hemicellulose material. Sugar composition determined by GC-FID (A) and xyloglucan fingerprint of the hemicellulose fraction isolated from non-infiltrated leaves by MALDI-TOF MS (B). Xyloglucan fingerprints of AIR isolated from Ni, water, p19 et H5 (C). Structure of XSGGG fragment (D). Nomenclature of xyloglucan fragments according to Fry *et al*. (1993). G: Glc residue carrying an acetate group.

Figure 5:

Callose detection. Gas chromatograms of the monosubstituted hexose regions (18.5-21 min) obtained after permethylation of AIR isolated from leaves collected at day 7 from control plants (Ni) and plants infiltrated with water or *Agrobacterium* strains (p19 and H5). 3-linked Glc results from callose deposition. 4-linked Glc corresponds to cellulose and 3-linked and 4-linked Gal arises from galactans.

Figure 6:

Lignin detection at day 1, 4 and 7 by staining with phloroglucinol. For each plant group, the leaves right side was infiltrated, whereas the left side was not.

Supplemental Figure 1:

MALDI-TOF MS/MS of m/z ion at 1331.7 assigned to XSGGG and its pattern of fragmentation.

Supplemental Table 1:

Monosaccharide compositions of AIR extracted from leaves collected at day 1, 4 and 7. nd: not detected.

Supplemental Table 2A:

Relative proportion of xyloglucan structures found by MALDI-TOF MS analysis of hemicellulose fraction treated by endoglucanase. nd: not detected, H: hexose, P: pentose.

Supplemental Table 2B:

Structure of xyloglucan fragments detected after endoglucanase treatment performed on AIR. H: hexose, P: pentose; A: Acetyl group; ?: Unknown structure; *: Structure confirmed by MS-MS analysis. Nomenclature for proposed structures: G: non substituted Glc unit, G: acetylated Glc, X: Glc substituted by α-D-Xyl*p*-(1→6) residue, S: Glc substituted by α-L-Ara*f*-(1→2)-α-D-Xylp-(1→6) side chain and T: Glc substituted by α-L-Ara*f*-(1→3)-α-L-Ara*f*-(1→2)-α-D-Xylp-(1→6) side chain.

Supplemental Table 2C:

Relative proportion of xyloglucan fragments detected after endoglucanase treatment performed on AIR. nd: not detected.

Figures:

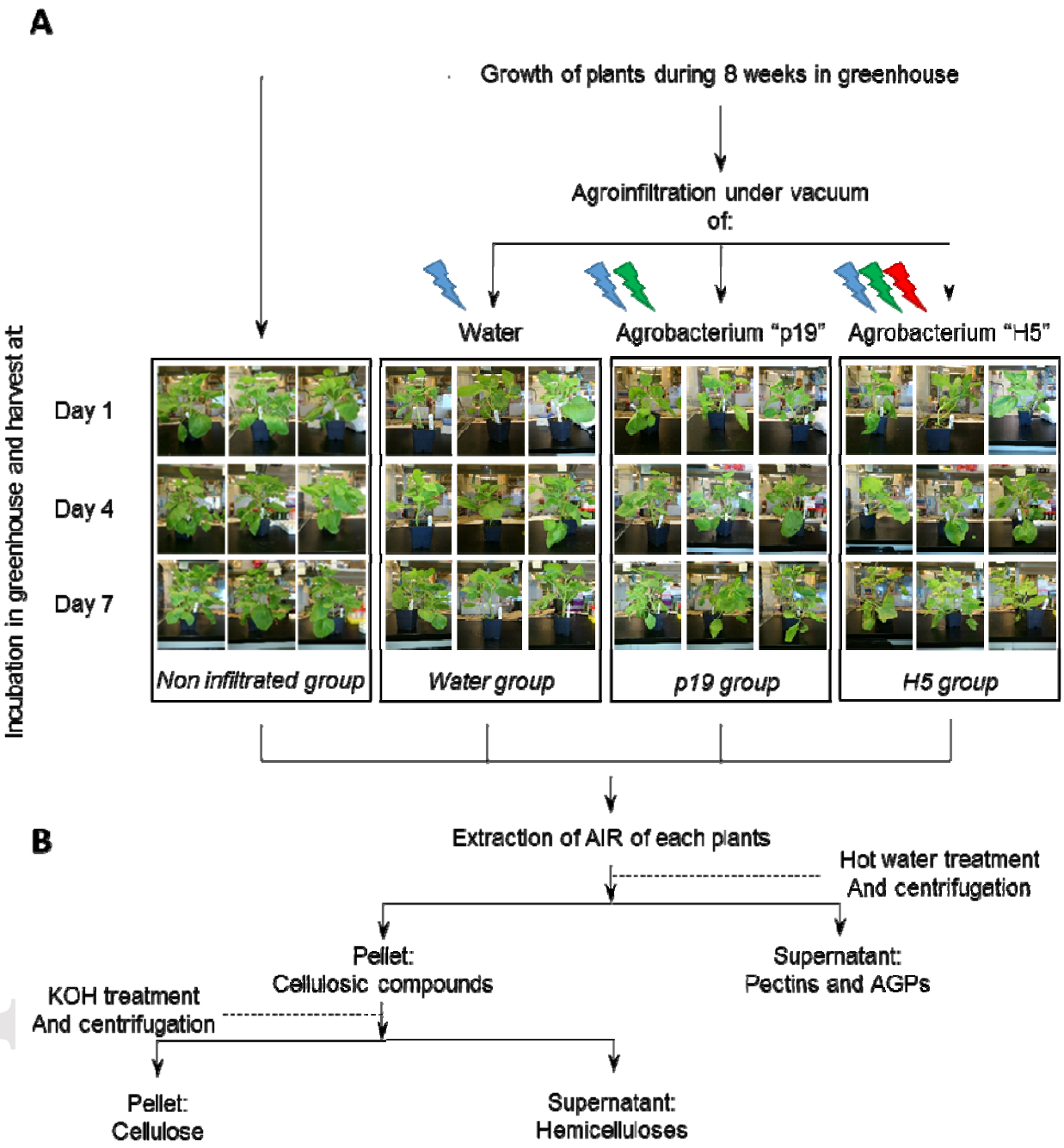

Figure 1. Experimental design of plants submitted to different biotic and abiotic treatments (A) and preparation of the cell wall constituents (B). Lightening icons represent the different stresses applied to each groups: abiotic stress from infiltration is in blue, biotic stress of bacterial infection is represented in green, and biotic stress arising from VLP production and accumulation is in red.

A

Day 1 Non infiltrated		
Ara	7.6%	±0.3%
Rha	15.9%	±1.9%
Fuc	0.3%	±0.1%
Xyl	8.7%	±0.7%
GlcA	2.0%	±1.4%
Man	2.1%	±0.3%
Gal	8.0%	±1.1%
GalA	22.4%	±3.7%
Glc	33.0%	±0.8%

B

Day 1 Non infiltrated	
Ara	t-Ara: 67%; 5-Ara: 32%
Rha	2-Rha: 66%; 2,4-Rha: 33%
Xyl	t-Xyl: 32%; 2 + 4-Xyl*: 68%
Gal	t-Gal: 12%; 3-Gal:11%; 4-Gal: 76%
Glc	4-Glc: 87%; 4,6-Glc: 13%

C

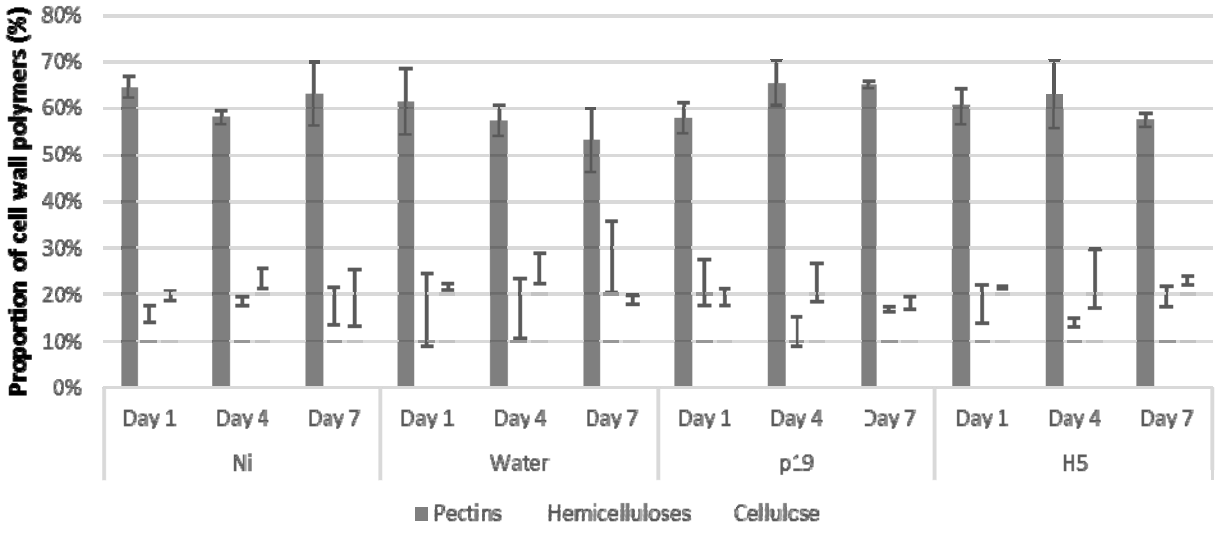

Figure 2. Analysis of AIR material. Sugar composition (A) and linkages (B) analysis of main neutral monosaccharides of AIR extracted from control leaves at day 1. *co-eluting partially O-methylated samples. Relative percentages of cell wall polysaccharide fractions from all conditions at Day 1, 4 and 7 (C). Ara: arabinose, Rha: rhamnose, Fuc: fucose, Xyl: xylose, GlcA: glucuronic acid, Man: mannose, GalA: galacturonic acid, Gal: galactose, Glc: glucose, t-: terminal.

A

Day 1 Non infiltrated		
Ara	12.7%	± 1.2%
Rha	18.6%	± 1.1%
Fuc	0.9%	± 0.1%
Xyl	1.5%	± 0.2%
GlcA	1.7%	± 0.6%
Man	1.9%	± 0.2%
Gal	16.6%	± 0.7%
GalA	46.1%	± 2.2%

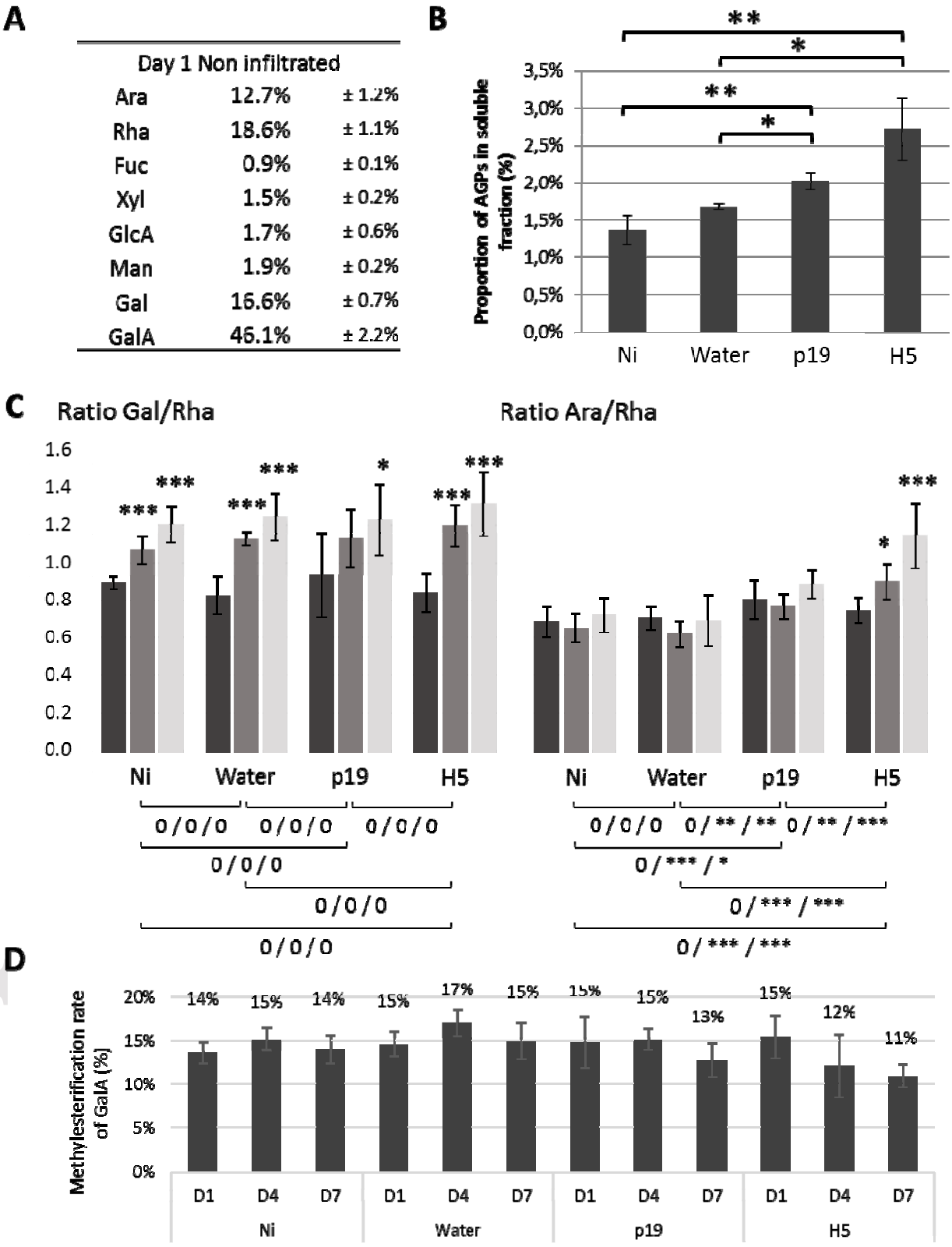

Figure3. Analysis of water soluble material. Monosaccharide composition of water soluble fraction of control plant at day 1 (A). Quantification of AGPs present in the water soluble fraction at day 7 (B). *: p-value below 0.05, **: p-value below 0.01 and

***: p-value below 0.001. Gal/Rha (left panel) and Ara/Rha ratio (right panel). Day 1 in black, day 4 in grey and day 7 in white. Symbols below charts indicate statistical analysis between the different conditions. First symbol corresponds to analysis performed on day 1, second one on day 4 and last one on day 7 (C). 0: no difference, *: p-value below 0.05, **: p-value below 0.01 and ***: p-value below 0.001. Degrees of methylesterification of pectins (D).

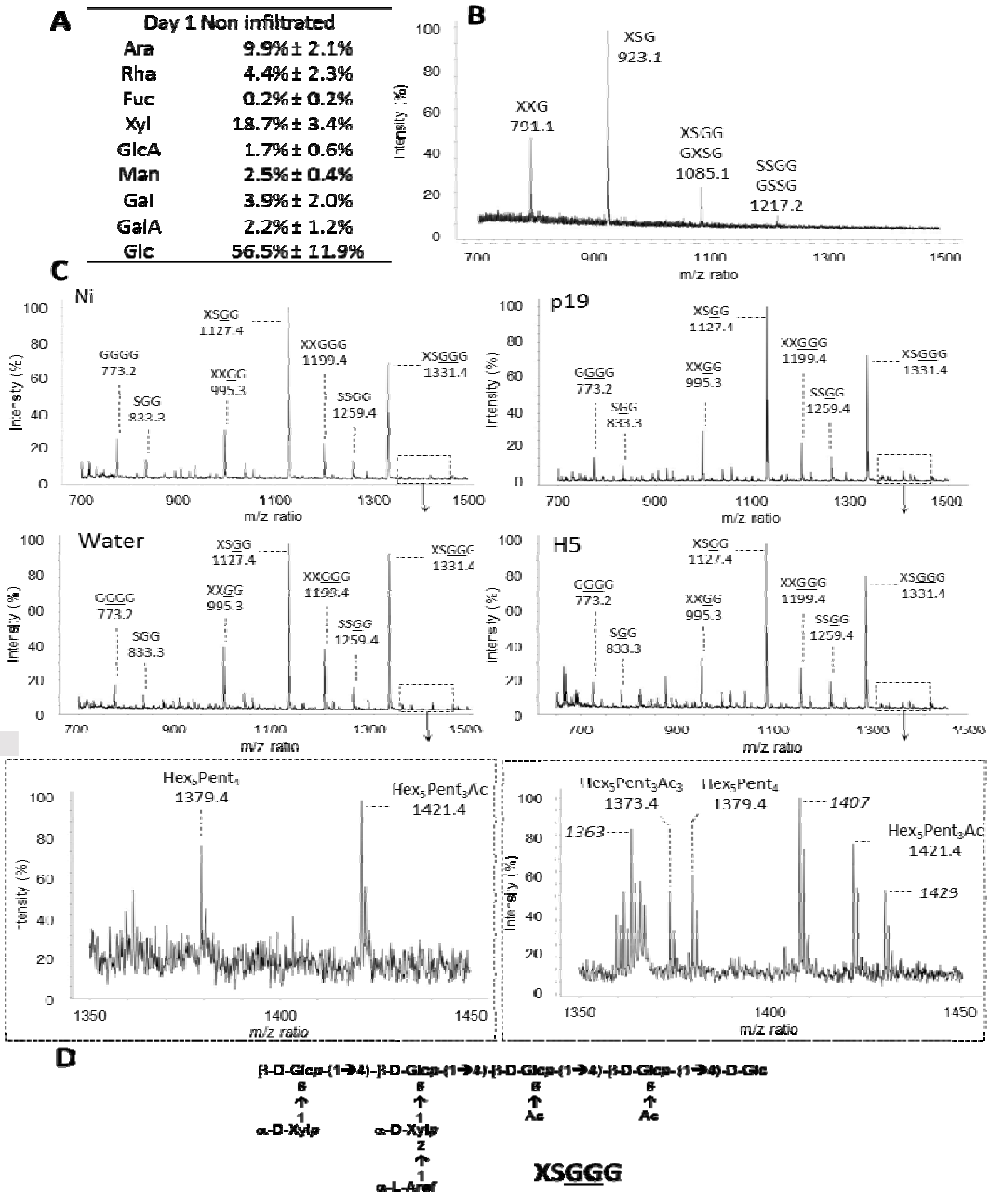

Figure 4. Analysis of hemicellulose material. Sugar composition determined by GC-FID (A) and xyloglucan fingerprint of the hemicellulose fraction isolated from non-infiltrated leaves by MALDI-TOF MS (B). Xyloglucan fingerprints of AIR isolated from Ni, water, p19 et H5 (C). Structure of XSGGG fragment (D). Nomenclature of xyloglucan fragments according to Fry *et al*. (1993). G: Glc residue carrying an acetate group.

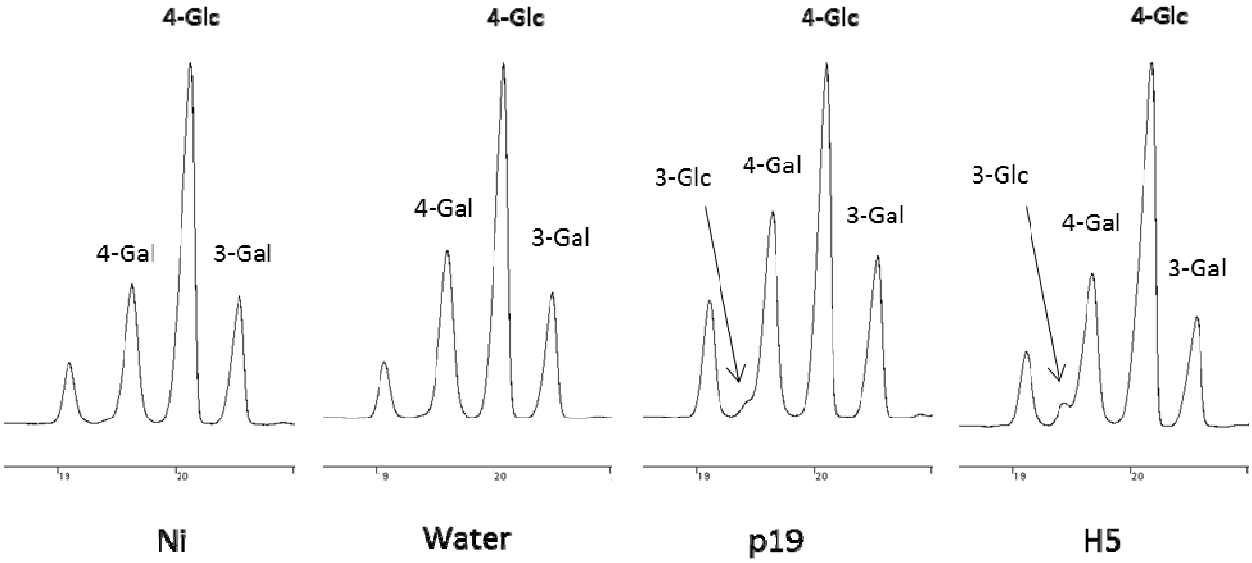

Figure 5. Callose detection. Gas chromatograms of the monosubstituted hexose regions (18.5-21 min) obtained after permethylation of AIR isolated from leaves collected at day 7 from control plants (Ni) and plants infiltrated with water or *Agrobacterium* strains (p19 and H5). 3-linked Glc results from callose deposition. 4-linked Glc corresponds to cellulose and 3-linked and 4-linked Gal arises from galactans.

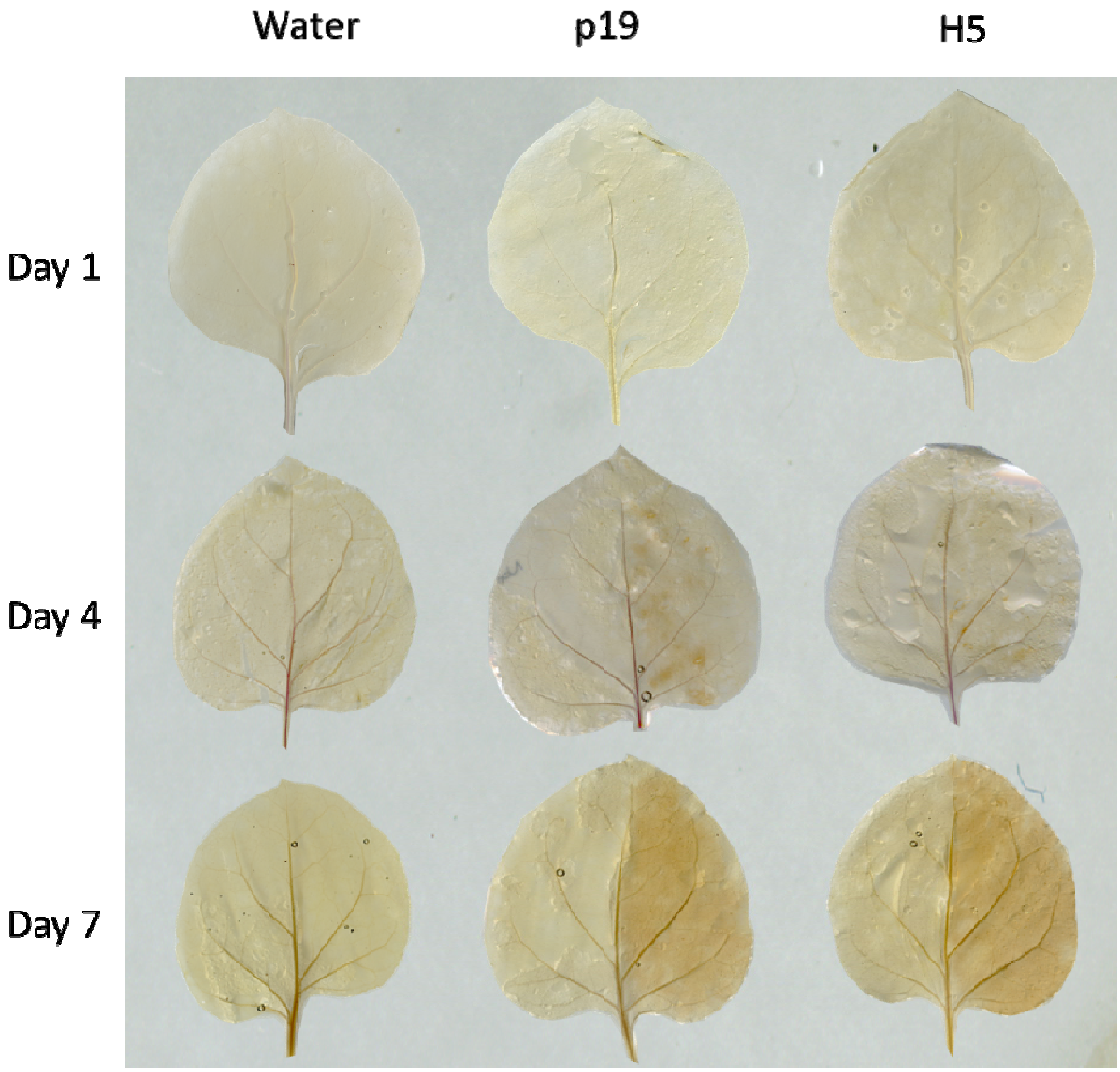

Figure 6. Lignin detection at day 1, 4 and 7 by staining with phloroglucinol. For each plant group, the leaves right side was infiltrated, whereas the left side was not.